

Polarized neutron reflectometry as a probe of nanoporous magnetic multilayers

B. J. Kirby,^{1, a)} M. T. Rahman,^{2,3} R. K. Dumas,^{4,5} J. E. Davies,⁶ C. H. Lai,² and Kai Liu⁴

¹⁾Center for Neutron Research, NIST, Gaithersburg, MD 20899, USA

²⁾Materials Science and Engineering, National Tsing Hua University, Hsinchu 30043, Taiwan

³⁾MINT Center, University of Minnesota, Minneapolis, MN 55455, USA

⁴⁾Physics Department, University of California, Davis, California 95616, USA

⁵⁾Physics, University of Gothenburg, Gothenburg 41296, Sweden

⁶⁾Advanced Technology Group, NVE Corporation, Eden Prairie, MN 55344, USA

(Dated: 22 August 2011)

We describe a polarized neutron reflectometry investigation of Co/Pt multilayers patterned via deposition onto nanoporous alumina host matrices. Despite the porosity and corresponding lack of in-plane uniformity or long-range order, we observe robust spin-dependent reflectivities, providing strong sensitivity to both the nuclear and magnetic depth profiles. The determined nuclear profiles show excellent agreement with cross-sectional transmission electron microscopy, consistent with uniform pore coverage. The magnetic profiles resolve distinct surface and subsurface magnetizations, and show an increase in sub-surface magnetization with increased sample porosity. These results pave the way for depth-resolved studies of novel magnetic multilayers systems with lateral dimensions controlled by methods that do not yield long-range in-plane order.

PACS numbers: 75.70.Cn, 78.70.Nx, 61.05.fj

Arrays of nanoscale magnetic elements not only have important applications in patterned recording media¹ and other spintronic devices,² but also facilitate fundamental studies of spatially confined magnetism.^{3,4} Deposition of magnetic multilayers onto porous host matrices has been shown as a simple and cost-effective method for achieving such arrays over macroscopic areas.^{5,6} For such structures, the magnetic properties are strongly influenced by patterning in the lateral direction as well as structural variations and magnetic coupling along the film depth. The amount of material deposited on top of the porous template (surface layer) vs. that inside the pores critically depends on the host pore aspect ratio $A = h/D$, where D is the pore diameter, and h is the pore depth. Along the lateral direction, the effect of patterning is manifested in the magnetization reversal mechanisms.⁵ On the other hand, resolving depth-dependent magnetic characteristics in such patterned nanostructures is much more challenging, as conventional magnetometry only gives the convoluted responses from all components. Polarized neutron reflectometry (PNR) is a technique that can provide such spatial resolution, but as it is sensitive to the in-plane average of the magnetic depth profile, it is most commonly used to study films or multilayers that are either compositionally continuous in the plane, or are patterned to exhibit long-range in-plane order. In this work we describe PNR measurements of samples that are highly heterogeneous in the plane, Co/Pt multilayers deposited on nanoporous alumina. These results demonstrate the utility of PNR

for resolving the structural and magnetic depth profiles of magnetic multilayers laterally confined by a porous matrix.

Nanoporous anodized alumina (AAO) matrices with pores of varying aspect ratio were produced by anodic oxidation of a 50 nm Al film on a Ti-capped Si substrate, and multilayers of 8 nm Pt seed / [0.5 nm Co / 2 nm Pt]₅ were deposited onto the porous matrices via dc magnetron sputtering.⁵ Transmission electron microscopy (TEM) showed that for templates with high A , most of the sputtered films were on top of the AAO; with decreasing A , more material was deposited on side walls of the pores, and eventually inside the pores. Magnetometry demonstrated that each of the samples as a whole exhibits strong perpendicular-to-plane magnetic anisotropy, with reversal behavior dependent on A . For this work, it is convenient to distinguish samples in terms of surface porosity p (the fraction of the surface covered by pores), as determined by TEM.⁵

PNR experiments were conducted using the NG1 Reflectometer at the NIST Center for Neutron Research. Of particular interest are two samples with $p \approx 11\%$ ($D \approx 13$ nm, $h \approx 41$ nm, $A \approx 3.2$), and $p \approx 53\%$ ($D \approx 28$ nm, $h \approx 20$ nm, $A \approx 0.7$). A monochromatic cold neutron beam was spin polarized up or down with respect to an applied magnetic field, and was incident on the sample. The specularly reflected beam was measured as a function of scattering vector Q_z using a point detector. Scans were conducted for spin-up and spin-down non-spin-flip scattering, and for spin-flip scattering. The obtained data were corrected for background, beam polarization, and beam footprint. No significant off-specular or spin-flip scattering was observed for any measurement, thus we discuss only the spin-up and spin-down non-spin-

^{a)}bkirby@nist.gov

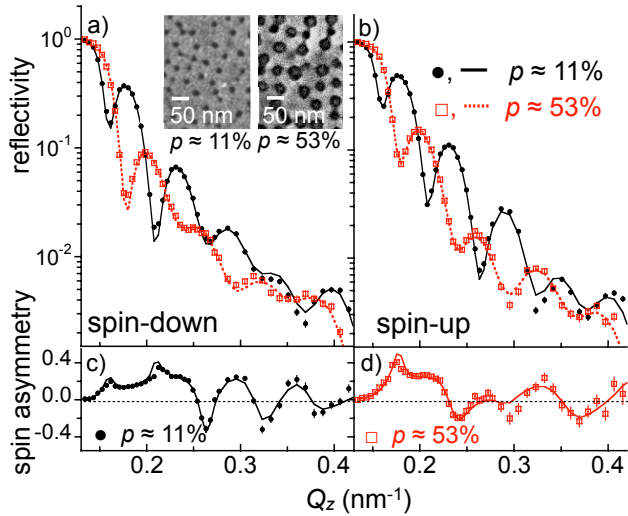


FIG. 1. Fitted spin-down (a), and spin-up (b) reflectivities for $p \approx 11\%$ and $p \approx 53\%$ samples. Panels c-d show the data and fits plotted as spin asymmetry. Error bars correspond to $\pm 1 \sigma$, and are smaller than the point size for much of the data shown. Insets are TEM images of the sample surfaces.

flip specular reflectivities. After saturating the samples along the sample normal direction, and then applying an 840 mT in-plane field, room temperature PNR measurements were conducted as a function of reduced field between 820-5 mT.

Specular PNR is sensitive to the nuclear and magnetic depth profiles of multilayer thin films, probing along the surface normal (z) direction while averaging over planar features.^{7,8} Specular reflection occurs at interfaces between regions with differing index of refraction (a function of nuclear composition and magnetization), and as such, sharp interfaces yield reflectivity features that are, in general, easier to detect and interpret. The porous samples in this study clearly deviate from this PNR ideal, illustrated by the plan-view TEM images of the samples, shown in the Fig. 1a inset. While there is a significant body of work showing the utility of PNR for characterization of patterned surfaces⁹⁻¹¹, such work has primarily focused on off-specular diffraction from large (μm scale) elements with long-range order. Although the cratered surfaces and non-discrete interfaces inherent to our porous samples present a challenge for specular PNR, we demonstrate that the technique is still a powerful probe of the buried magnetic and nuclear structure. A key point is that the pore diameters are 3-4 orders of magnitude smaller than the in-plane neutron coherence length for this experiment.¹² Thus, each neutron interacts with both porous and non-porous regions, and the specular scattering is representative of the average in-plane composition as a function of depth. While indiscrete interfaces are also non-ideal, previous work has demonstrated the utility of PNR for characterizing magnetic samples with highly graded interfaces.^{13,14}

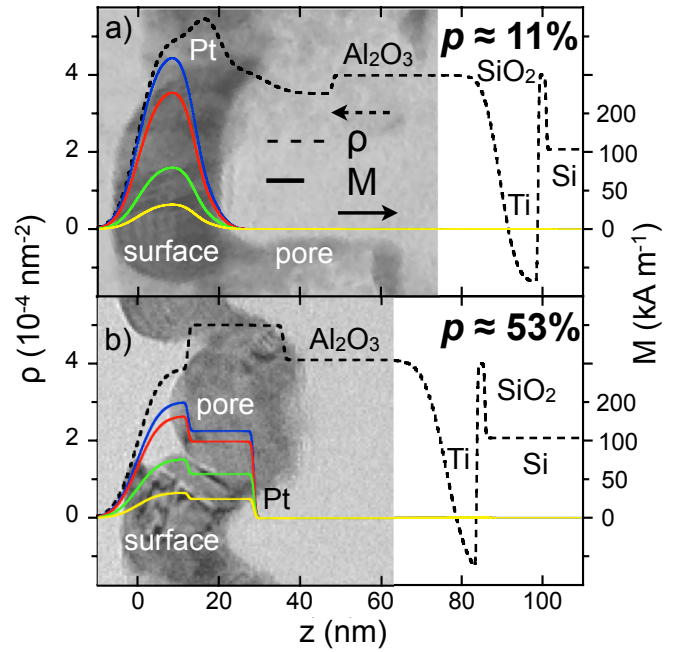


FIG. 2. Nuclear (dashed, left axis) and field-dependent magnetic (solid, right axis) depth profiles for $p \approx 11\%$ (a), and $p \approx 53\%$ (b) samples. For each sample, from top to bottom, the four magnetic profiles correspond to 820, 400, 100, and 5 mT, respectively.

Fig. 1 shows the low Q_z spin-down (a) and spin-up (b) reflectivities for each sample, measured in an in-plane field of 820 mT, clearly demonstrating the sensitivity to depth profiles of these porous samples. The pronounced oscillations indicate interfaces discrete enough to be distinguished, while sample-dependent differences demonstrate sensitivity to variations in porosity. The spin-down (-) and spin-up (+) reflectivities are functions of the scattering length density depth profile $\rho^\pm(z) = \rho_N \pm \rho_M$,^{7,8} where the nuclear component $\rho_N = \sum_i N_i b_i$ (where the N is the number density, b is the isotope characteristic scattering length¹⁵, and the summation is over each isotope in the system), and the magnetic component $\rho_M = CM$ (where M is the in-plane projection of the sample magnetization parallel to the applied field, and C is a constant¹⁶). Therefore, the sample magnetization is manifest as a splitting between the spin-up and spin-down reflectivities - a quantity displayed in Fig. 1 c-d by plotting the reflectivity data as spin asymmetry = (spin-up - spin-down) / (spin-up + spin-down). For both porosities, a clearly oscillating, non-zero spin asymmetry is observed, establishing a sensitivity to the magnetic depth profiles of these porous layers.

Model-fitting of the data in Fig. 1 (lines) and lower field data (not shown) using exact dynamical calculations^{7,8} reveals the nuclear (dashed lines) and field-dependent magnetic (solid lines) scattering length density profiles of the samples, shown in Fig. 2. From

top to bottom, the magnetic profiles correspond to fields of 820, 400, 100, and 5 mT, respectively. Scaled cross-sectional TEM images from Ref. 5 are shown in the background, and show excellent agreement with the nuclear profiles. Rather than confining the models to a guessed number of expected layers, the approach taken here is to freely vary parameters in the profile, while using the fewest possible layers that can account for the data.¹⁷ While our primary interest is in the porous Co/Pt multilayer near the sample surface, the highly penetrating neutron beam is sensitive to the entire sample, including the non-porous portion of the Al₂O₃ and the Ti adhesion layer, both of which contribute strongly to the scattering. The profiles for these near-substrate regions are similar for both samples, with ρ_N that agree well with expected values¹⁸, except for that of the non-porous alumina base, which is reduced by approximately 25% (likely indicating reduced density due to the anodization process).

The PNR data are also quite sensitive to porous multilayer regions of the samples. Since the Q_z range being probed is well below where we would be sensitive to the individual Co and Pt layers in the multilayer stacks ($Q_z \approx 2.5 \text{ nm}^{-2}$) those multilayers are treated collectively as Co_{0.2}Pt_{0.8} alloys.^{19,20} The ρ_N values of Co ($2.2 \times 10^{-4} \text{ nm}^{-2}$) and Pt ($6.3 \times 10^{-4} \text{ nm}^{-2}$) are known,¹⁸ thus to facilitate interpretation of the porous surface regions, we define a porosity corrected expected nuclear scattering length density $\rho' = (1-p)\rho_N$, where $\rho_N = 5.5 \times 10^{-4} \text{ nm}^{-2}$ is the expected value for Co_{0.2}Pt_{0.8}.

For the $p \approx 11\%$ sample (Fig. 2a), the surface region ρ_N is consistent with the expected $\rho' = 4.9 \times 10^{-4} \text{ nm}^{-2}$, evidence that the porosity determined by TEM is indeed representative of the average over the entire surface. The round edges for the magnetic profiles in this surface region are highly consistent with the curved multilayers indicated by TEM, and are also consistent with strongly exchange coupled magnetic components. Moving right from the surface region, there is an increase in ρ_N corresponding to the depth of the porous Pt seed, followed by a region of non-magnetic, slowly decreasing ρ_N , indicative of seed layer Pt that dripped down the alumina pore walls. As only the surface region shows any magnetization, we can conclude that the sample's net magnetic moment (as would be measured in a standard magnetometer) is indeed indicative of the patterned multilayer surface.

The $p \approx 53\%$ sample (Fig. 2b) is significantly different, with profiles indicative of a surface network of multilayers perforated by completely filled, strongly magnetized pores. For this sample, the surface ρ_N is significantly larger than the expected $\rho' = 2.6 \times 10^{-4} \text{ nm}^{-2}$ - indicating that in the cross-sectional average being probed, we are sensitive to significant overlap between surface multilayers, and multilayers within the pores. The abrupt increase (decrease) in nuclear (magnetic) ρ near $z \approx 15 \text{ nm}$ corresponds to the bottom of the surface Co/Pt multilayer deposited on top of the AAO. Materials at depths of $30 > z > 15 \text{ nm}$ correspond to Co/Pt multilayers de-

posited at the bottom of the pores, averaged with the surface multilayer's Pt seed layer (at lower z) and the AAO matrix (at higher z). The two-step magnetic profile evident in Fig. 2b shows that the net magnetic moment of this sample does not correspond to a single multilayer, but is instead a convolution of moment originating from Co/Pt stacked on the AAO surface and that stacked inside the pores. These two components are physically and magnetically decoupled, in contrast to the $p \approx 11\%$ sample which shows largely a single magnetic component with a continuous magnetic depth profile (Fig. 2a). For both samples, the agreement between the ρ_N profiles and the TEM images is excellent, a strong validation of the fitting results.

In summary, we have used PNR to resolve the nuclear and magnetic depth profiles of a series of Co/Pt multilayers deposited onto nanoporous AAO templates with different aspect ratio and porosity. The nuclear profiles agree well with TEM images, and are consistent with a uniform porosity across the sample surface. The magnetic profiles resolve surface and subsurface contributions to the net magnetization, and show a clear increase in sub-surface magnetization with increased porosity (decreased pore aspect ratio). These results demonstrate the utility of PNR for investigation of porous magnetic media, and pave the way for future studies of novel magnetic multilayers tuned by confinement in a porous matrix.

Support from the NSF Materials World Network program (DMR-1008791) is gratefully acknowledged. We thank J. A. Borchers, B. B. Maranville, and C. F. Majkrzak of NIST for valuable discussions.

- ¹O. Hellwig, A. Moser, E. Dobisz, Z. Z. Bandic, H. Yang, D. S. Kercher, J. D. Risner-Jamtgaard, D. Yaney, and E. E. Fullerton, *Appl. Phys. Lett.* **93**, 192501 (2008).
- ²S. Mangin, D. Ravelosona, J. A. Katine, M. J. Carey, B. D. Terris, and E. E. Fullerton, *Nature Materials* **5**, 210 (2006).
- ³L. J. Heyderman, F. Nolting, D. Backes, S. Czekaĳ, L. Lopez-Diaz, M. Klauĳ, U. Rudiger, C. A. F. Vaz, J. A. C. Bland, R. J. Matelon, U. G. Volkman, and P. Fischer, *Phys. Rev. B* **73**, 214429 (2006).
- ⁴K. Liu, S. M. Baker, M. Tuominen, T. P. Russell, and I. K. Schuller, *Phys. Rev. B* **63**, 060403 (2001).
- ⁵M. T. Rahman, R. K. Dumas, N. N. Shams, Y.-C. Wu, K. Liu, and C. H. Lai, *Appl. Phys. Lett.* **94**, 042507 (2009).
- ⁶M. T. Rahman, N. N. Shams, C. H. Lai, J. Fidler, and D. Suess, *Phys. Rev. B* **81**, 014418 (2010).
- ⁷C. F. Majkrzak, *Physica B* **221B**, 342 (1996).
- ⁸C. F. Majkrzak, K. V. O'Donovan, and N. F. Berk, in *Neutron Scattering from Magnetic Materials*, edited by T. Chatterji (Elsevier Science, New York, 2005).
- ⁹H. Fritzsche, M. J. V. Bael, and K. Temst, *Langmuir* **19**, 7789 (2003).
- ¹⁰S. Langridge, L. A. Michez, M. Ali, C. H. Marrows, B. J. Hickey, T. R. Charlton, R. M. Dalgliesh, M. Toohey, E. W. Hill, S. McFadzean, and J. N. Chapman, *Physical Review B* **19**, 014417 (2006).
- ¹¹K. L. Krycka, B. B. Maranville, J. A. Borchers, F. J. Castano, B. G. Ng, J. C. Perkinson, and C. A. Ross, *J. Appl. Phys.* **105**, 07C120 (2009).
- ¹²C. Metting, B. B. Maranville, J. A. Dura, and C. M. Majkrzak, to be published (2011).
- ¹³B. J. Kirby, J. A. Borchers, J. J. Rhyne, S. G. E. te Velhuis,

- A. Hoffmann, K. V. O'Donovan, T. Wojtowicz, X. Liu, W. L. Lim, and J. K. Furdyna, *Phys. Rev. B* **69**, 081307 (2004).
- ¹⁴R. K. Dumas, Y. Fang, B. J. Kirby, C. Zha, V. Bonanni, J. Nogues, and J. Åkerman, *Physical Review B* **84**, 054434 (2011).
- ¹⁵in *International Tables for Crystallography* (Wiley, Hoboken, New Jersey, New York, 2006) Chap. 4.4, p. 430.
- ¹⁶ $C = 2.853 \times 10^{-7}$, for M in kA m^{-1} and ρ_M in nm^{-2} .
- ¹⁷The native oxide layer is an exception - 2 nm of SiO_2 layer are assumed to be present.
- ¹⁸M. R. Fitzsimmons and C. F. Majkrzak, in *Modern Techniques for Characterizing Magnetic Materials*, edited by Z. Zhu (Kluwer, New York, 2005).
- ¹⁹B. J. Kirby, S. M. Watson, J. E. Davies, G. T. Zimanyi, K. Liu, R. D. Shull, and J. A. Borchers, *J. Appl. Phys.* **105**, 07C929 (2009).
- ²⁰B. J. Kirby, J. E. Davies, K. Liu, S. M. Watson, G. T. Zimanyi, R. D. Shull, P. A. Kienle, and J. A. Borchers, *Phys. Rev. B* **81**, 100405 (2010).